Minimum-Time Travel for a Vehicle with Acceleration Limits: Theoretical Analysis and Receding Horizon Implementation

Efstathios Velenis* and Panagiotis Tsiotras†

To appear in the Journal of Optimization Theory and Applications

Abstract

A methodology is proposed to generate minimum-time optimal velocity profiles for a vehicle with prescribed acceleration limits along a specified path. The necessary optimality conditions are explicitly derived, allowing the construction of the optimal solution semi-analytically. A receding horizon implementation is also proposed for the on-line implementation of the velocity optimizer. Robustness of the receding horizon algorithm is guaranteed by the use of an adaptive scheme that determines the planning and execution horizons. Application to a real-life scenario with a comparison between the infinite and finite receding horizon schemes provides a validation of the proposed methodology.

Keywords: minimum time velocity profile, acceleration limits, receding horizon.

1 Introduction

The problem of trajectory planning for high-speed autonomous vehicles is typically dealt with in the literature by means of numerical optimization. Several published results have addressed path planning of high-speed ground vehicles [1, 2, 3, 4]. These results demonstrate that numerical techniques allow one to incorporate accurate, high order dynamical models in the optimization process, thus producing realistic results. In fact, the optimal solutions generated using these optimizers are comparable to experimental results obtained from expert race drivers [2, 3, 4]. On the other hand, these numerical optimization approaches are computationally intensive, and they cannot be readily applied in cases where the environment changes unpredictably. As a result, they are not suitable for real-time path-planning optimization. In the work of Spenko [5] real-time trajectory planning for hazard avoidance of high-speed Unmanned Ground Vehicles (UGV's) in rough terrain has been addressed. A fairly rich vehicle model has been used to predict and avoid roll-over and excessive side-slip. The computational cost is mitigated somewhat by choosing the hazard avoidance maneuver from a library of off-line pre-computed candidates.

An alternative approach for on-line trajectory optimization of ground vehicles is proposed in this work. Having in mind the requirement for reduction of the computational cost, we explore the possibility of solving the trajectory planning problem (or at least part of this problem) analytically or semi-analytically. We separate the geometric problem of designing the optimal path from the dynamic

*Postdoctoral Fellow, D. Guggenheim School of Aerospace Engineering, Georgia Institute of Technology, ev18@mail.gatech.edu.

†Professor, D. Guggenheim School of Aerospace Engineering, Georgia Institute of Technology, p.tsiotras@ae.gatech.edu.

[1]This work has been supported in part by the US Army Research Office, award numbers DAAD19-00-1-0473 and W911NF-05-1-0331. The authors would also like to thank an anonymous reviewer for his insightful comments regarding the results in Section 5.

problem of optimally following this path given the vehicle dynamic characteristics. This separation of the geometric from the dynamic problem has also been proposed in [6, 7] and [8].

A similar problem to the one investigated in this paper has been addressed in [9, 10] and [11]. Therein the authors investigated the minimum time solution for a robotic manipulator moving its tip along a prescribed path, while taking into consideration the actuator limits. In order for all actuators to maintain enough control authority for the tip to track the desired path *exactly*, a state constraint is introduced which defines a set of admissible velocities. Proof of optimality is provided by point-wise maximization of the velocity.

In this work we first provide a rigorous proof of optimality of the approach in [6, 7, 8] using optimal control theory. The effect of limited accelerating/braking and cornering forces due to tire friction saturation is explicitly accounted for. The set of admissible velocities is explicitly expressed in terms of the acceleration capacity of the vehicle and the curvature of the path to be followed. A constructive proof of optimality for several special cases of paths to be followed is provided. The necessary optimality conditions are explicitly derived, which allow us to draw conclusions on the number and type of control switchings. An application to an F1 circuit provides a validation of the proposed methodology. We also propose a receding horizon implementation of the previous semi-analytical optimal velocity profile algorithm. The algorithm ensures that at the end of each executed subarc the vehicle can reach a "safe state" (for example, complete stop) regardless of the (a priori unknown) changes in the environment outside the planning horizon. This is achieved by designing a dynamic scheme that determines appropriate planning and execution horizons. Finally, we apply the receding horizon optimization scheme to an F1 circuit to validate our approach.

2 Problem Statement

Consider a vehicle of mass m traveling along a prescribed path, with given acceleration limits and fixed initial and final position and velocity. The path is described by a parameterized planar curve in terms of its radius $r(s)$ (or curvature $k(s) \triangleq 1/r(s)$) as a function of the arc length s.

Assuming a point-mass model for the vehicle, the equations of motion are given by

$$m\frac{\mathrm{d}^2 s}{\mathrm{d}t^2} = f_t, \qquad m\left(\frac{\mathrm{d}s}{\mathrm{d}t}\right)^2 = f_n r(s), \tag{1}$$

where, f_t is the tangential component of the force along the path, and f_n is the normal (centripetal) force such that the vehicle tracks the prescribed path. In this work we will assume that the force acting on the vehicle is limited within the set defined by the inequalities

$$\begin{aligned} \left(\frac{f_t}{f_t^{\max}}\right)^2 + \left(\frac{f_n}{f_n^{\max}}\right)^2 - 1 \le 0, \qquad f_t > 0, \\ \left(\frac{f_t}{f_t^{\min}}\right)^2 + \left(\frac{f_n}{f_n^{\max}}\right)^2 - 1 \le 0, \qquad f_t < 0, \end{aligned} \tag{2}$$

where $f_t^{\max} > 0$ and $f_t^{\min} < 0$. For the case when $f_t^{\min} = -f_t^{\max}$ the inequalities (2) describe the ellipse

$$\left(\frac{f_t}{f_t^{\max}}\right)^2 + \left(\frac{f_n}{f_n^{\max}}\right)^2 - 1 \le 0, \tag{3}$$

where $f_t^{\max}$ is the maximum longitudinal force and $f_n^{\max}$ is the maximum lateral force. These forces are mainly due to the friction forces at the tires, but they may also include other effects such as the effect of aerodynamic forces.

We assume that the initial and final vehicle velocities are given, and satisfy

$$\left.\frac{\mathrm{d}s}{\mathrm{d}t}\right|_{t=t_0} < \frac{f_n^{\max} r(s_0)}{m}, \qquad \left.\frac{\mathrm{d}s}{\mathrm{d}t}\right|_{t=t_f} \le \frac{f_n^{\max} r(s_f)}{m}, \tag{4}$$

in order for the initial and final cornering forces to be less than the allowable limit $f_n^{\max}$ and also in order for some accelerating/braking force f_t to be available at t_0. Moreover, it will be assumed that the velocity of the vehicle is always greater than or equal to zero, that is, $\mathrm{d}s/\mathrm{d}t \geq 0$ for all $t \in [t_0, t_f]$. Specifically, the vehicle is not allowed to reverse direction, a natural assumption for a minimum-time problem.

2.1 A State Transformation

Consider equations (1) with $\mathrm{d}s/\mathrm{d}t \triangleq v$. We have

$$m\dot{v} = f_t, \qquad mv^2 = f_n r(s). \tag{5}$$

Using the second of the previous equation, we have the following constraint on the tangential force

$$f_t^{\min}\sqrt{1-\left(\frac{mv^2}{r(s)f_n^{\max}}\right)^2} \leq f_t \leq f_t^{\max}\sqrt{1-\left(\frac{mv^2}{r(s)f_n^{\max}}\right)^2}. \tag{6}$$

The first equation in (5) can then be written as

$$\dot{v} = \tilde{u}\sqrt{1-\left(\frac{v^2}{\tilde{r}(s)}\right)^2}, \qquad \tilde{u} \in \left[\frac{f_t^{\min}}{m}, \frac{f_t^{\max}}{m}\right] \tag{7}$$

where $\tilde{r}(s) \triangleq r(s)f_n^{\max}/m$. If we assume $f_t^{\min} = -f_t^{\max}$ we may define

$$z_1 \triangleq \frac{m}{f_t^{\max}}s, \qquad z_2 \triangleq \frac{m}{f_t^{\max}}v, \tag{8}$$

in which case the state equations may be written as

$$\dot{z}_1 = z_2, \qquad \dot{z}_2 = \frac{f_t}{f_t^{\max}} = u\sqrt{1-\left(\frac{z_2^2}{R(z_1)}\right)^2}, \qquad u \in [-1, +1], \tag{9}$$

where

$$R(z_1) \triangleq \left(\frac{m}{f_t^{\max}}\right)^2 \tilde{r}((f_t^{\max}/m)z_1). \tag{10}$$

From now on, and unless stated otherwise, we assume symmetric acceleration and deceleration limits. This assumption can be made without loss of generality and it results in simplified formulas. Indeed, if $f_t^{\min} \neq -f_t^{\max}$ one may resort to equations (7) which have the same form as (9) where now $u \in [u_{\min}, u_{\max}]$.

2.2 Feasibility Region

The model in (9) describing the dynamics of the problem is well defined only for trajectories inside the region $\mathcal{S} \subset \mathbb{R}^2$ of the state space defined by

$$\mathcal{S} \triangleq \{(z_1, z_2) : C_0(z_1, z_2) \triangleq z_2^2 - |R(z_1)| \leq 0\}. \tag{11}$$

The right-hand side of (9) is not Lipschitz continuous when $C_0(z_1, z_2) = 0$ and there exists the possibility of multiple solutions emanating from the manifold $C_0(z_1, z_2) = 0$. Furthermore, controllability is maintained only at the interior of the set $\mathcal{S}$. At the boundary of the set $\mathcal{S}$ controllability of equation (9) is lost. We will study in greater detail the case $C_0(z_1, z_2) = 0$ in Section 5. For the time being, we will assume that all trajectories lie in the interior of the set $\mathcal{S}$.

The following lemma states that unless we have a path of constant curvature, the state constraint $C_0(z_1, z_2) \leq 0$ is always inactive for any finite interval of time. In the following, $R'(z_1) = \partial R(z_1)/\partial z_1$.

Lemma 2.1 *Assume $R'(z_1) \neq 0$ for any $z_1 \in (z_\alpha, z_\beta) \subset [z_{10}, z_{1f}]$, where $z_{10} = z_1(\tau_0)$ and $z_{1f} = z_1(\tau_f)$. Then the manifold $\partial\mathcal{S} = \{(z_1, z_2) : C_0(z_1, z_2) = 0\}$ is not invariant for the system (9) for any control u.*

Proof: Invariance of $\partial\mathcal{S}$ with respect to (9) implies that $-\dot{z}_1 R'(z_1)\ \mathrm{sgn}R(z_1) + 2z_2\dot{z}_2 = 0$, equivalently, $-z_2 R'(z_1)\ \mathrm{sgn}R(z_1) = 0$, since $\dot{z}_2 = 0$ on $\partial\mathcal{S}$ for any $u \in [-1, +1]$. Since $z_2 > 0$ for all $z_1 \in (z_{10}, z_{1f})$, the last equation is satisfied if and only if $R'(z_1) = 0$. ■

An immediate consequence of Lemma 2.1 is the fact that $\partial\mathcal{S}$ may be invariant under (9) only for paths of constant curvature (see Section 5). At this point note that the flow of the trajectories of (9) in the vicinity of the constraint $C_0(z_1, z_2) = 0$ are given by

$$\frac{\mathrm{d}C_0(z_1, z_2)}{\mathrm{d}t} = \frac{\partial C_0}{\partial z_1}\dot{z}_1 + \frac{\partial C_0}{\partial z_2}\dot{z}_2 = -z_2 R'(z_1)\ \mathrm{sgn}R(z_1).$$

The following corollary is therefore immediate.

Corollary 2.1 *The set $\mathcal{S}$ is invariant for the system (9) only for paths of monotonically decreasing curvature (increasing radius). Such paths are characterized by the inequality $R'(z_1)\,\mathrm{sgn}R(z_1) > 0$.*

Given a certain path, characterized by its radius $R(z_1)$, the velocity z_2 for which the constraint $C_0(z_1, z_2) = 0$ is satisfied is thus of extreme importance for our problem. We will denote this velocity by $z_{2\mathrm{crit}}(z_1)$. It is given by

$$z_{2\mathrm{crit}}(z_1) \triangleq \sqrt{|R(z_1)|}. \tag{12}$$

When $z_2(z_1) = z_{2\mathrm{crit}}(z_1)$ for some $z_1 \in [z_{10}, z_{1f}]$ loss of controllability ensues. Corollary 2.1 essentially states that for paths of monotonically decreasing curvature loss of controllability can occur only instantaneously.

We know turn to the solution of the minimum time problem for system (9).

3 Optimal Control Formulation

In reference to the system (9), and given fixed initial conditions $z_{10} = z_1$, $z_{20} = z_2$ at $\tau = \tau_0$ and final condition $z_{1f} = z_1$, $z_{2f} = z_2$ at $\tau = \tau_f$, we desire the optimal control u that drives the system (9) from point A to point B of the cartesian plane in minimum time τ_f subject to (11). We adopt the notation z_1^P and z_2^P for the path length coordinate z_1 and velocity z_2 of a point P of the prescribed path $R(z_1)$. Thus, we have $z_1^A = z_{10}$, $z_2^A = z_{20}$, $z_1^B = z_{1f}$ and $z_2^B = z_{2f}$. Notice that without loss of generality we may assume that $z_2(\tau) > 0,\ \forall\ \tau \in (\tau_0, \tau_f)$.

The cost function to be minimized is written as

$$J = \int_{\tau_0}^{\tau_f} \mathrm{d}\sigma. \tag{13}$$

The Hamiltonian for this problem is

$$H(z, \lambda, u) = 1 + \lambda_1 z_2 + \lambda_2 u\sqrt{1 - \left(\frac{z_2^4}{R^2(z_1)}\right)} + \mu C_0(z_1, z_2). \tag{14}$$

The system of adjoint equations is

$$\dot{\lambda}_1 = -\frac{\partial H}{\partial z_1} = -\lambda_2 u \frac{z_2^4}{\sqrt{1 - z_2^4/R^2(z_1)}}\frac{R'(z_1)}{R^3(z_1)} + \mu\ \mathrm{sgn}R(z_1)R'(z_1), \tag{15}$$

$$\dot{\lambda}_2 = -\frac{\partial H}{\partial z_2} = -\lambda_1 + 2\lambda_2 u \frac{z_2^3}{R^2(z_1)\sqrt{1 - z_2^4/R^2(z_1)}} - 2z_2\mu. \tag{16}$$

The Kuhn-Tucker conditions imply

$$\mu = 0 \text{ for } C_0(z_1, z_2) < 0 \quad \text{and} \quad \mu \geq 0 \text{ for } C_0(z_1, z_2) = 0. \tag{17}$$

The transversality condition implies $H(\tau_f) = 0$, and since the Hamiltonian does not depend explicitly on time, it also follows that

$$H(\tau) = 0, \quad \forall\ \tau \in [\tau_0, \tau_f]. \tag{18}$$

Consider first the case of an inactive constraint, $C_0(z_1, z_2) < 0$. In this case $\mu = 0$ and Pontryagin's Maximum Principle leads to the optimal control

$$u^* = \text{argmin}_{u\in[-1,+1]} H(z, \lambda, u) = \begin{cases} -1 \text{ for } \lambda_2 > 0, \\ +1 \text{ for } \lambda_2 < 0, \end{cases} \tag{19}$$

which implies,

$$u^*(\tau) = -\operatorname{sgn} \lambda_2(\tau). \tag{20}$$

Therefore λ_2 is the switching function, which determines the value of u^*.

Let us consider the possibility of a singular control interval in the optimal solution, i.e., the existence of a time interval $(\tau_1, \tau_2) \subset [\tau_0, \tau_f]$ such that $\lambda_2(\tau) = 0$, for all $\tau \in (\tau_1, \tau_2)$. Equation (15) implies that $\dot{\lambda}_1(\tau) = 0$ for all $\tau \in (\tau_1, \tau_2)$, or equivalently $\lambda_1(\tau) = \lambda_{10} =$ constant for all $\tau \in (\tau_1, \tau_2)$. Equation (16) implies $\dot{\lambda}_2(\tau) = -\lambda_{10}\tau$ for all $\tau \in (\tau_1, \tau_2)$. In addition, $\lambda_2(\tau) = 0$ and $\dot{\lambda}_2(\tau) = 0$ for all $\tau \in (\tau_1, \tau_2)$, and thus we have $\lambda_{10} = 0$ and $\lambda_1(\tau) = \lambda_2(\tau) = 0$ for all $\tau \in (\tau_1, \tau_2)$. Equation (14) then gives $H(\tau) = 1$ for $\tau \in (\tau_1, \tau_2)$, which contradicts the condition (18) that $H(\tau) = 0$ for all $\tau \in [\tau_0, \tau_f]$.

We have thus proven the following proposition.

Proposition 3.1 *Assuming that throughout the optimal trajectory $C_0(z_1, z_2) < 0$, there can be no singular subarc.*

4 Solution for Special Cases of Path Curvature: Inactive Constraint

In the following, we provide solutions to the previous minimum-time problem for several special cases of $R(z_1)$. First, we consider the simplest case when the constraint (11) remains inactive. We distinguish three different cases: paths of monotonically decreasing curvature, paths of constant curvature and paths of monotonically increasing curvature.

4.1 Path of Decreasing Curvature

Consider a path of monotonically decreasing curvature from point A to point B in the cartesian plane denoted by

$$\mathcal{P}^+_{AB} = \left\{(z_1, R(z_1)) :\ R'(z_1)\operatorname{sgn}R(z_1) > 0,\ z_1 \in [z_1^A, z_1^B]\right\}. \tag{21}$$

From Proposition 3.1 we know that the optimal path is composed solely of subarcs of maximum acceleration or maximum deceleration.

Equation (15) with $R'(z_1)\operatorname{sgn}R(z_1) > 0$ yields $\dot{\lambda}_1(\tau) \geq 0$, for all $\tau \in [\tau_0, \tau_f]$. Suppose now that there exists a switching time $\tau_1 \in (\tau_0, \tau_f)$. It follows that $\lambda_2(\tau_1) = 0$. The transversality condition (18) implies $\lambda_1(\tau_1) = -1/z_2(\tau_1)$. For any $\tau \in [\tau_0, \tau_1)$ we have that

$$-\frac{1}{z_2(\tau)} \leq \frac{-1 + |\lambda_2|\sqrt{1 - z_2^4/R^2(z_1)}}{z_2(\tau)} = \lambda_1(\tau) \leq \lambda_1(\tau_1) = -\frac{1}{z_2(\tau_1)} \tag{22}$$

since λ_1 is non-decreasing. Inequality (22) implies that $z_2(\tau) \leq z_2(\tau_1)$ for all $\tau \in [\tau_0, \tau_1)$, from which we conclude that τ_1 is a switching point from $u = +1$ to $u = -1$.

Following the same steps as for the switching point τ_1, it is easy to prove that any other switching point $\tau_2 \in (\tau_0, \tau_1)$ has to be from $u = +1$ to $u = -1$. Obviously, there can be no consecutive switching points from $u = +1$ to $u = -1$ without a switching from $u = -1$ to $u = +1$ in between. Thus, we rule out the possibility of existence of a second switching point $\tau_2 \in (\tau_0, \tau_1)$. Finally, suppose that there exists a switching point $\tau_3 \in (\tau_1, \tau_f)$. The transversality condition (18) implies $\lambda_1(\tau_3) = -1/z_2(\tau_3)$. Since λ_1 is non-decreasing we have that $\lambda_1(\tau_1) \leq \lambda_1(\tau_3)$ or that $-1/z_2(\tau_1) \leq -1/z_2(\tau_3)$ and finally that $z_2(\tau_1) \leq z_2(\tau_3)$, implying that the vehicle accelerates from τ_1 to τ_3, which contradicts the fact that $u(\tau) = -1$ for $\tau \in (\tau_1, \tau_3)$. It follows that we can have only one switching in the control.

Let now $Z_A^+(z_1)$ be the characteristic constructed by forward integration of (9) from (z_1^A, z_2^A) with $u = +1$, and $Z_B^-(z_1)$ be the characteristic constructed by backward integration of (9) from (z_1^B, z_2^B) with $u = -1$. We have therefore the following proposition for the optimal trajectory on paths of monotonically decreasing curvature.

Proposition 4.1 *In the case of a path of monotonically decreasing curvature $\mathcal{P}_{AB}^+$ there can be at most one switching in the control, from $u = +1$ to $u = -1$. In this case the optimal solution is given by $z_2^*(z_1) = \min\left\{Z_A^+(z_1), Z_B^-(z_1)\right\}$.*

It is easy to prove the optimality of the previous strategy directly by showing that $z_2^*(z_1)$ maximizes the velocity pointwise for all $z_1 \in [z_1^A, z_1^B]$.

4.2 Path of Constant Curvature

Consider a path of constant curvature from point A to point B, denoted by

$$\mathcal{P}_{AB}^0 = \left\{(z_1, R(z_1)) : \ R'(z_1) = 0, \ z_1 \in [z_1^A, z_1^B]\right\}. \tag{23}$$

According to Lemma 2.1, the constraint (11) may remain active only for a path of constant curvature. Following the same steps as in Section 4.1, one can show the following result.

Proposition 4.2 *In case of a path of constant curvature $\mathcal{P}_{AB}^0$, assuming that $C_0(z_1, z_2) < 0$, there can be at most one switching in the control, from $u = +1$ to $u = -1$. In this case the optimal solution is given by $z_2^*(z_1) = \min\left\{Z_A^+(z_1), Z_B^-(z_1)\right\}$.*

4.3 Path of Increasing Curvature

Consider a path of monotonically increasing curvature from point A to point B denoted in the cartesian plane by

$$\mathcal{P}_{AB}^- = \left\{(z_1, R(z_1)) : \ R'(z_1)\,\mathrm{sgn}R(z_1) < 0, \ z_1 \in [z_1^A, z_1^B]\right\}. \tag{24}$$

Similar to the case of a path of decreasing curvature, the optimal path is composed only of subarcs of maximum acceleration or maximum deceleration, assuming that the optimal trajectories remain in the interior of $\mathcal{S}$ (Proposition 3.1). An analysis similar to the one of Section 4.1 can be followed to show that, assuming the trajectories remain in $\mathcal{S}$, there can be at most one switch in the control, from $u = +1$ to $u = -1$. Below we show that the optimal trajectory does indeed remain in $\mathcal{S}$.

As before, let $Z_A^+(z_1)$ be the characteristic constructed by forward integration of (9) from (z_1^A, z_2^A) with $u = +1$, and $Z_B^-(z_1)$ be the characteristic constructed by backward integration of (9) from (z_1^B, z_2^B) with $u = -1$.

Lemma 4.1 *Assuming $z_2^B \le z_{2\text{crit}}(z_1^B)$, then $Z_B^-(z_1) < z_{2\text{crit}}(z_1)$ for all $z_1 \in [z_1^A, z_1^B)$.*

Proof: The proof involves two steps. First, we construct the locus $\mathcal{M}$ of points in the z_1-z_2 plane having the following property: the slope of any trajectory beginning from any point in $\mathcal{M} \subset \mathcal{S}$ using the control $u = -1$ is less than or equal to the slope of $z_{2\text{crit}}(z_1)$. In the second step we show that for characteristic path starting in $\mathcal{S}\backslash\mathcal{M}$ constructed by backward integration of (9) with $u = -1$ remains in $\mathcal{S}$.

To this end, note that the smallest possible slope in the z_1-z_2 plane of any feasible trajectory is achieved using maximum deceleration ($u = -1$). In particular, we have

$$\dot{z}_2 = u\sqrt{1 - \frac{z_2^4}{R^2(z_1)}} \Rightarrow z_2' = \frac{u}{z_2}\sqrt{1 - \frac{z_2^4}{R^2(z_1)}}, \tag{25}$$

which for $u = -1$ yields $z'_{2\min} = -1/z_2\sqrt{1 - z_2^4/R^2(z_1)}$. On the other hand, the slope of the $z_{2\text{crit}}(z_1)$ characteristic in (12) is $z'_{2\text{crit}}(z_1) = \text{sgn}R(z_1)R'(z_1)/2\sqrt{|R(z_1)|} \triangleq \rho(z_1)$. We may therefore enforce the inequality $z'_{2\min} \le z'_{2\text{crit}}$ by

$$P(z_2) \triangleq z_2^4 + R^2(z_1)\rho^2(z_1)z_2^2 - R^2(z_1) \le 0. \tag{26}$$

Solving for z_2^2, the roots of $P(z_2)$ are

$$r_{1,2} \triangleq \frac{-R^2(z_1)\rho^2 \mp \sqrt{R(z_1)^4\rho^4 + 4R^2(z_1)}}{2}, \tag{27}$$

and for (26) to hold, given $z_2 > 0$, we must have

$$z_2 \le \sqrt{r_2} = \left(\frac{-R^2(z_1)\rho^2(z_1) + \sqrt{R^4(z_1)\rho^4(z_1) + 4R^2(z_1)}}{2}\right)^{1/2}. \tag{28}$$

In the limiting case, when $z'_{2\min} = z'_{2\text{crit}}$, we have $z_{2\text{safe}} = \sqrt{r_2}$. An explicit relationship between $z_{2\text{safe}}$ and $z_{2\text{crit}}$ is given by the equation

$$z_{2\text{safe}}^4 - z_{2\text{crit}}^4 + \left(\frac{R'(z_1)^2}{4}\right) z_{2\text{safe}}^2 z_{2\text{crit}}^2 = 0, \tag{29}$$

which implies that $z_{2\text{safe}}(z_1) < z_{2\text{crit}}(z_1)$ for all $z_1 \in [z_1^A, z_2^B]$. The set $\mathcal{M}$ is therefore the area underneath the curve $z_{2\text{safe}}(z_1)$. It follows that $\mathcal{M} \subset \mathcal{S}$. The $z_{2\text{crit}}(z_1)$ and $z_{2\text{safe}}(z_1)$ curves for paths of increasing curvature are shown in Fig. 1.

To complete the proof, notice that for any trajectory starting in $\mathcal{S}\backslash\mathcal{M}$ (the area between the characteristics $z_{2\text{safe}}(z_1)$ and $z_{2\text{crit}}(z_1)$ in Fig. 1) using $u = -1$, we have that $z'_{2\min} > z'_{2\text{crit}}$. Integrating now backwards in time from z_1^B to z_1 ($\text{d}z_1 < 0$) using $u = -1$ one obtains

$$\int_{z_1^B}^{z_1} \text{d}z_{2\min} < \int_{z_1^B}^{z_1} \text{d}z_{2\text{crit}}, \tag{30}$$

or $z_{2\min}(z_1) - z_{2\min}(z_1^B) < z_{2\text{crit}}(z_1) - z_{2\text{crit}}(z_1^B)$. Since $z_{2\min}(z_1^B) \le z_{2\text{crit}}(z_1^B)$ for points in $\mathcal{S}\backslash\mathcal{M}$ it follows that $z_{2\min}(z_1) < z_{2\text{crit}}(z_1)$. We conclude that for an increasing curvature path $\mathcal{P}_{AB}^-$, we have $Z_B^-(z_1) < z_{2\text{crit}}(z_1)$ for all $z_1 \in [z_1^A, z_1^B)$, given that $z_2^B \le z_{2\text{crit}}(z_1^B)$. ■

Lemma 4.1 implies, in particular, that $z_2(z_1) = \min\left\{Z_A^+(z_1), Z_B^-(z_1)\right\} < z_{2\text{crit}}(z_1)$ for $z_1 \in [z_1^A, z_1^B)$. Hence the constraint (11) remains inactive throughout the optimal trajectory. We have therefore shown the following result for the optimal trajectory on paths of monotonically increasing curvature.

Proposition 4.3 *In the case of a path of monotonically decreasing curvature $\mathcal{P}_{AB}^-$, there can be at most one switching in the control, from $u = +1$ to $u = -1$. In this case the optimal solution is given by $z_2^*(z_1) = \min\left\{Z_A^+(z_1), Z_B^-(z_1)\right\}$.*

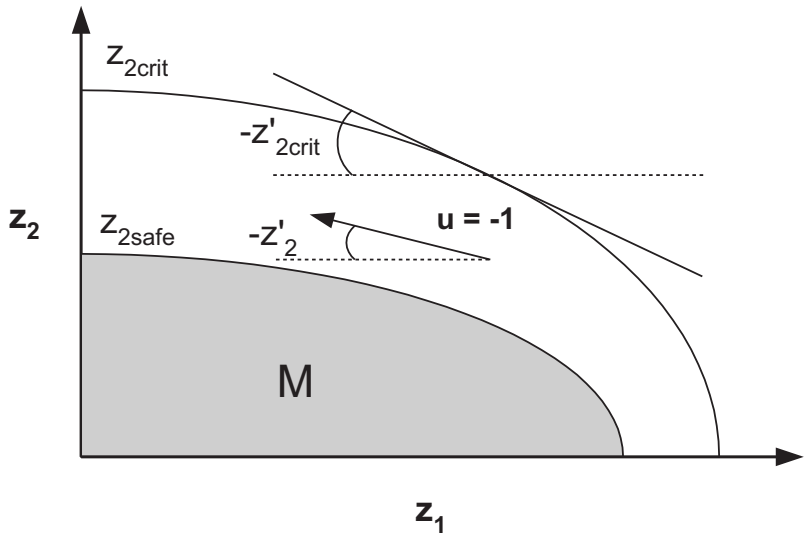

Figure 1: In the area between $z_{2\text{crit}}$ and $z_{2\text{safe}}$ we can integrate backward in time with $u = -1$ without intersecting $z_{2\text{crit}}$.

5 Solution for Special Cases of Path Curvature: Active Constraint

In this section we consider the case when the constraint (11) is active, i.e., $C_0(z_1, z_2) = 0$. From Lemma 2.1 it follows that this case is possible only for paths of constant curvature. In the remaining of this section we will therefore consider only paths with $R'(z_1) = 0$.

To this end, consider a path of constant curvature $\mathcal{P}^0_{AF}$. Figure 2(a) shows the characteristic $Z^+_A(z_1)$ constructed by forward integration of (9) from (z_1^A, z_2^A) with $u = +1$, the characteristic $z_{2\text{crit}}(z_1)$, and the characteristic $Z^-_F(z_1)$ constructed by backward integration of (9) from (z_1^F, z_2^F) with $u = -1$. Notice that $z_{2\text{crit}}(z_1)$ is constant in this case. This is easily seen from the fact that $C_0(z_1, z_2) = 0$ implies $\dot{z}_2 = 0$.

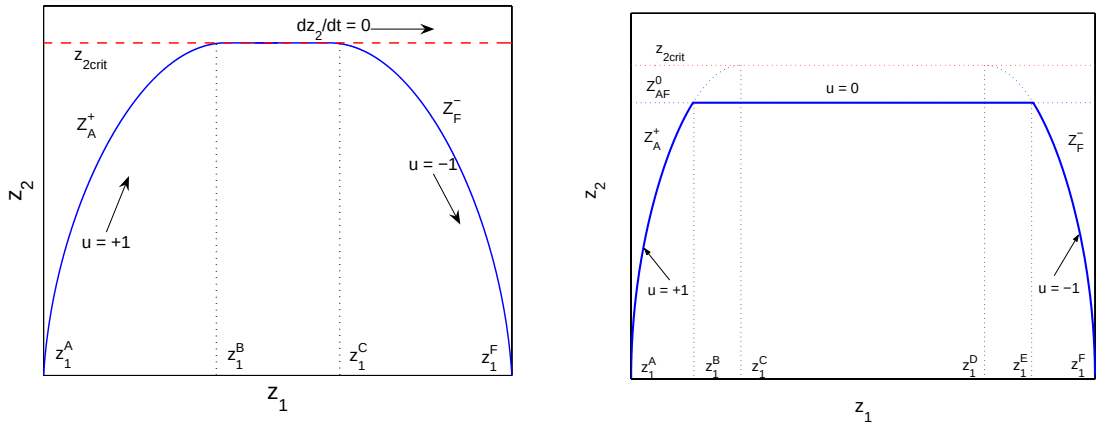

Figure 2: Constant radius path; active constraint case.

To investigate the properties of the trajectory when the constraint (11) is active (this is the part of the trajectory from $(z_1^B, z_{2\text{crit}})$ to $(z_1^C, z_{2\text{crit}})$ in Figure 2(a)) we return to equation (9), which we now rewrite as

$$\dot{z}_1 = z_2, \qquad \dot{z}_2 = z_3 \tag{31}$$

where $z_3 \triangleq f_t / f_t^{\max}$ satisfies

$$z_3^2 = 1 - \left(\frac{z_2^2}{R(z_1)} \right)^2. \tag{32}$$

The previous equation implies that maximum allowable acceleration or deceleration is used throughout the path according to the optimality conditions. By taking the derivative of (32) one obtains

$$2 z_3 \dot{z}_3 = -4 \frac{z_2^3}{R^2(z_1)} \dot{z}_2 = -4 \frac{z_2^3}{R^2(z_1)} z_3 \tag{33}$$

and, assuming $z_3 \neq 0$, one obtains the following differential equation for z_3

$$\dot{z}_3 = -2 \frac{z_2^3}{R^2(z_1)}. \tag{34}$$

Equations (31) and (34) are satisfied everywhere along a path of constant curvature, except when $z_2 = z_{2\text{crit}}$. For $z_2 = z_{2\text{crit}}$ equation (32) is trivially satisfied with $z_3 = \dot{z}_3 = 0$.

The overall trajectory can now be constructed as shown in Figure 2(a). We have thus shown the following proposition.

Proposition 5.1 *In the case of a path of constant curvature $\mathcal{P}_{AF}^0$ the optimal solution is given by* $z_2^*(z_1) = \min \left\{ Z_A^+(z_1), z_{2\text{crit}}(z_1), Z_F^-(z_1) \right\}$.

The optimality of the proposed strategy can also be shown by using a limiting argument as follows. To this end, we introduce the constraint

$$C_\epsilon(z_1, z_2) \triangleq z_2^2 + \epsilon - |R(z_1)| = 0, \tag{35}$$

where $\epsilon > 0$ is a small positive scalar. We investigate optimal paths that satisfy this constraint and then we take $\epsilon \to 0$ to recover the case of $C_0(z_1, z_2) = 0$ at the limit.

An easy calculation shows that the control law that keeps the vehicle on the constraint (35) is given by

$$u_{\text{sc}} = \frac{R(z_1) R'(z_1)}{2\sqrt{2|R(z_1)|\epsilon - \epsilon^2}}, \tag{36}$$

which, upon $R'(z_1) = 0$ yields $u_{\text{sc}} \equiv 0$ for any $\epsilon > 0$. Hence $\lim_{\epsilon \to 0} u_{\text{sc}} = 0$.

Figure 2(b) shows the characteristic $Z_A^+(z_1)$ constructed by forward integration of (9) from (z_1^A, z_2^A) with $u = +1$, the characteristic $Z_{AF}^0(z_1)$ given by $z_2(z_1) = \sqrt{|R(z_1)| - \epsilon} < z_{2\text{crit}}(z_1)$, for $z_1 \in [z_1^A, z_1^F]$, with $\epsilon > 0$, and the characteristic $Z_F^-(z_1)$ constructed by backward integration of (9) from (z_1^F, z_2^F) with $u = -1$. Notice that the characteristic $Z_{AF}^0(z_1)$ is constructed with $u = 0$, which coincides with u_{sc} in (36) for $R'(z_1) = 0$. On the characteristic $Z_{AF}^0(z_1)$ the constraint (35) remains active, i.e., $C_\epsilon(z_1, Z_{AF}^0(z_1)) = 0$.

Proposition 5.2 *In the case of a path of constant curvature $\mathcal{P}_{AF}^0$, assuming $\epsilon \geq 0$, the optimal solution is given by* $z_2^*(z_1) = \min \left\{ Z_A^+(z_1), Z_{AF}^0(z_1), Z_F^-(z_1) \right\}$.

Remark 5.1 Notice that equation (9) is not Lipschitz continuous, and the possibility of multiple solutions arises. This is, in fact, evident from Figure 2(a), where two solutions emanate from the point $(z_1^C, z_{2\text{crit}})$. The first solution is to trivially follow the characteristic $z_2 \equiv z_{2\text{crit}}(z_1)$. The second solution is to follow $Z_F^-(z_1)$. The latter is the optimal one since it also satisfies the final boundary condition. Note that if $z_1^F = z_{2\text{crit}}$ the two solutions coincide.

In the sequel we investigate paths composed of concatenations of paths investigated thus far. Such concatenations will allow us to construct the optimal trajectories, along with the corresponding optimal controls, by piecing together the solutions provided by Propositions 3.1-5.1.

6 Path with $\min R(z_1)$

Consider now a path of increasing curvature $\mathcal{P}_{AC}^-$ followed by a path of decreasing curvature $\mathcal{P}_{CB}^+$ as in Fig. 3. We adopt the following notation for the path from point A to point B

$$\begin{aligned}\mathcal{P}_{ACB}^{\mp} = \mathcal{P}_{AC}^- \circ \mathcal{P}_{CB}^+ \quad = \quad & \left\{(z_1, R(z_1)) : R'(z_1)\,\text{sgn}R(z_1) < 0,\ z_1 \in [z_1^A, z_1^C),\right. \\ & \left. R'(z_1)\,\text{sgn}R(z_1) > 0,\ z_1 \in [z_1^C, z_1^B])\right\}, \end{aligned} \tag{37}$$

where "$\circ$" denotes the concatenation operator. The function $R(z_1)$ has a minimum at z_1^C (see Fig. 3).

Let $z_2^*(z_1)$ denote the minimum time solution from A to B and z_2^{C*} denote the velocity at point C of the $z_2^*(z_1)$ trajectory. According to Bellman's Principle of Optimality if the solution $A \to B$ is optimal then the first part of this solution, $A \to C$, solves the minimum time problem from A to C with the final condition $z_2(\tau_f) = z_2^{C*}$. Similarly, the second part, $C \to B$, solves the minimum-time problem from C to B with initial condition $z_2(\tau_0) = z_2^{C*}$.

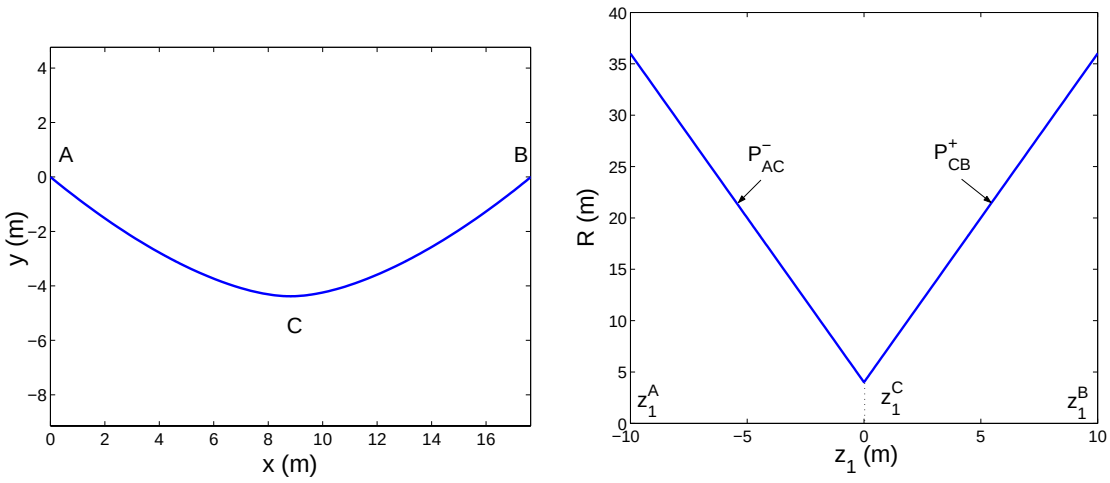

Figure 3: Path with minimum radius at point C, in cartesian coordinates (left); path radius as a function of path length (right).

On the part $A \to C$ we have a path of increasing radius, and according to Section 4.1 the possible optimal velocity profiles, summarized in Fig. 4(a), are: $u = +1$ (Case 1), $u = -1$ (Case 2) or $u = +1$ that switches once to $u = -1$ (Case 3). Similarly, on the part $C \to B$ we have a path of decreasing radius and according to Section 4.3 the possible optimal velocity profiles, summarized in Fig. 4(b), are: $u = +1$ (Case a), $u = -1$ (Case b) or $u = +1$ that switches once to $u = -1$ (Case c). For Bellman's Principle of Optimality to hold, the overall solution from A to B will consist of the subarcs $A \to C$ and $C \to B$ that correspond to Cases 1,2,3 and Cases a,b,c (Fig 4), respectively. Thus, all the possible

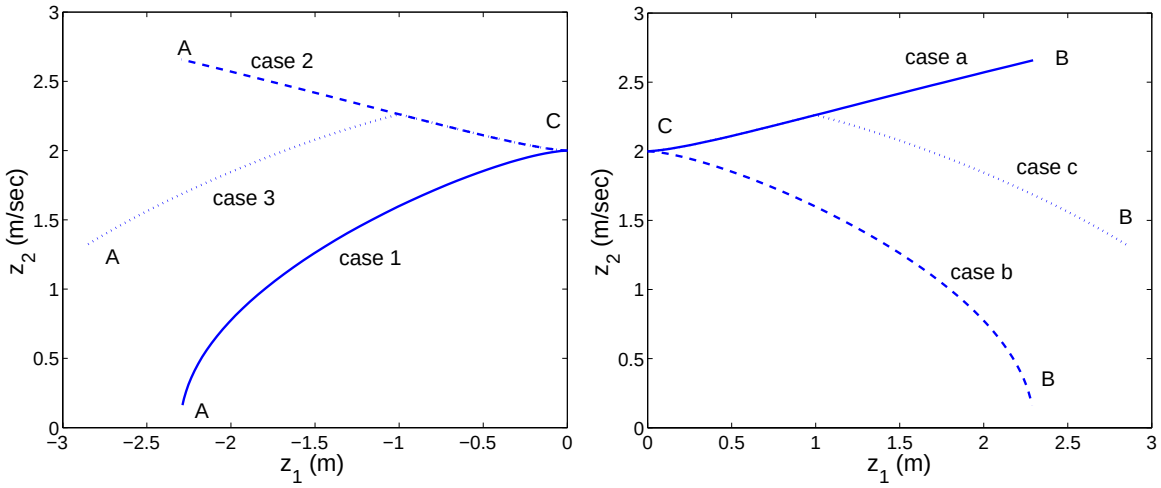

(a) $A \to C$ (b) $C \to B$

Figure 4: Possible optimal velocity profiles before (left) and after (right) point C.

optimal velocity profiles for the overall problem from A to B are all the possible combinations of Cases 1,2,3 and Cases a,b,c. These are shown in Fig 5.

There are only two possible scenarios for the value of z_2^{C*}. In Cases 1a, 2a, 3a, 2b and 3b we have $z_2^{C*} \leq z_{2\text{crit}}(z_1^C)$ and z_{2C}^* is determined by satisfying the boundary conditions of A and B using allowable control switches. In Cases 2a, 2c, 3a and 3c we have $z_2^{C*} = z_{2\text{crit}}(z_1^C)$ and a control switch from $u = -1$ to $u = +1$ at C.

Next, we propose a methodology to construct the overall optimal solution for a path with curvature switching from increasing to decreasing at a point C. Starting from (z_1^A, z_2^A) we construct the characteristic $Z_A^+(z_1)$ integrating the equations of motion (9) forward in time using $u = +1$. Starting from (z_1^B, z_2^B) we construct the characteristic $Z_B^-(z_1)$ integrating the equations of motion (9) backward in time using $u = -1$. Starting from $(z_1^C, z_{2\text{crit}}(z_1^C))$ we construct the characteristic $Z_C^-(z_1)$ integrating the equations of motion (9) backward in time using $u = -1$. Finally, starting from $(z_1^C, z_{2\text{crit}}(z_1^C))$ we construct the characteristic $Z_C^+(z_1)$ integrating the equations of motion (9) forward in time using $u = +1$. The optimal velocity profile is then given by $z_2^*(z_1) = \min\left\{Z_A^+(z_1), Z_C^-(z_1), Z_C^+(z_1), Z_B^-(z_1)\right\}$. It is easy to show that the previous strategy reproduces all the cases of Fig. 5.

7 Path with $\max R(z_1)$

Consider now a path of decreasing curvature $\mathcal{P}_{AC}^+$ followed by a path of increasing curvature $\mathcal{P}_{CB}^-$. We adopt the following notation for the path from point A to point B

$$\mathcal{P}_{ACB}^{\pm} = \mathcal{P}_{AC}^+ \circ \mathcal{P}_{CB}^-. \tag{38}$$

Clearly, in this case the function $R(z_1)$ has a maximum at z_1^C. All possible scenarios that may appear along the subarcs $A \to C$ and $C \to B$ according to the solutions presented in Sections 4.1 and 4.3 may be summarized in accordance to Fig. 4.

In Section 6 we concluded that Cases 2a, 2c, 3a and 3c may appear as the optimal solutions only if the velocity at C is $z_2^{C*} = z_{2\text{crit}}(z_1^C)$. Since C is a point of maximum radius, the critical velocity at point C is larger compared to any other point from A to B. That is, $z_{2\text{crit}}(z_1) < z_{2\text{crit}}(z_1^C)$ for $z_1 \in [z_1^A, z_1^C) \cup (z_1^C, z_1^B]$. On the other hand, in Cases 2a, 2c, 3a and 3c the velocity at point C is a local minimum. In this case we have that $z_2(z_1) > z_{2\text{crit}}(z_1)$ for all z_1 in a small enough neighborhood of z_1^C

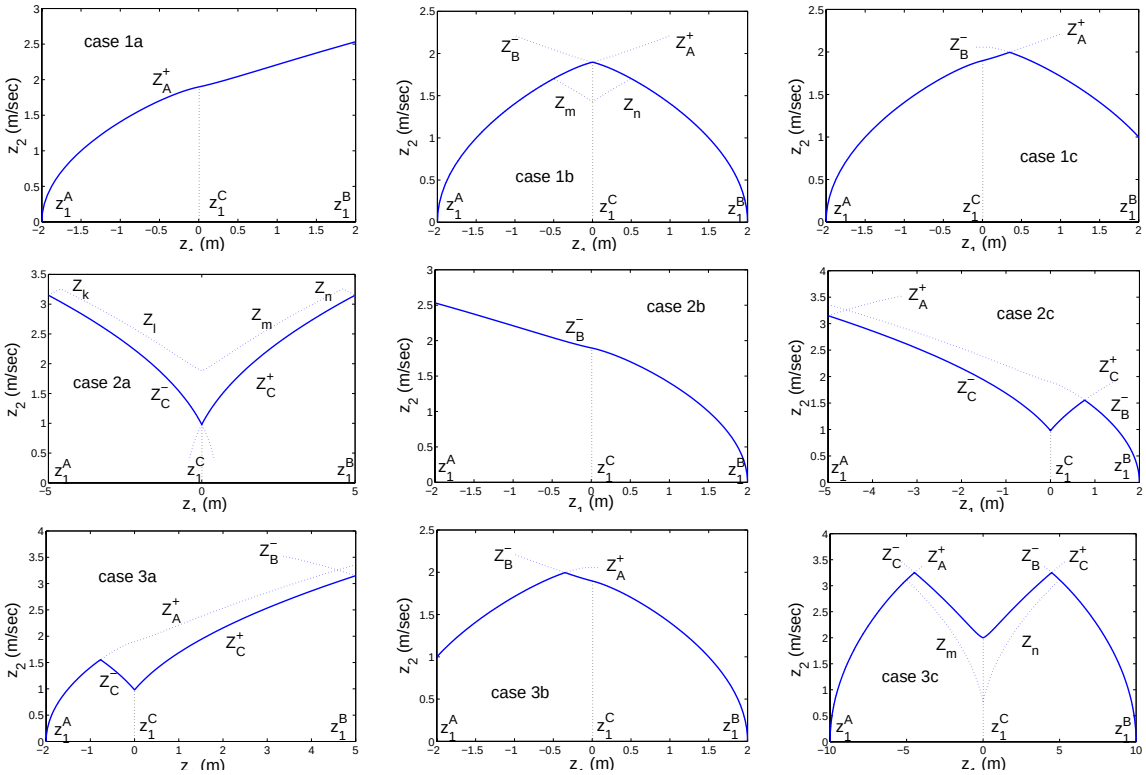

Figure 5: All possible optimal velocity profiles from A to B.

and the vehicle cannot follow the prescribed path. We conclude that Cases 2a, 2c, 3a and 3c cannot appear as optimal solutions in the case of a path with a point C of maximum radius.

The only possible scenarios are Cases 1a, 1b, 1c, 2b and 3b, where the optimal velocity at C is determined by the initial and final boundary conditions. The optimal solution is finally given by $z_2^*(z_1) = \min\left\{Z_A^+(z_1), Z_B^-(z_1)\right\}$.

8 General Solution

Assume that the given path from point A to point B is composed of a finite number of segments of constant curvature, of segments of monotonically increasing curvature and segments of monotonically decreasing curvature. Let the total number of segments be $n+1$. The path from point A to point B can then be expressed as

$$\mathcal{P}_{AB} = \mathcal{P}_{AP_1}^{i_1} \circ \mathcal{P}_{P_1P_2}^{i_2} \circ \mathcal{P}_{P_2P_3}^{i_3} \circ \cdots \circ \mathcal{P}_{P_nB}^{i_{n+1}}, \tag{39}$$

where $i_k \in \{+,\ -,\ 0\},\ k = 1, 2, ..., n+1$.

Let $\mathcal{I}^{\mp}$ denote the set of indices corresponding to points of minimum radius of the path $\mathcal{P}_{AB}$, that is, $\mathcal{I}^{\mp} = \{j : i_j = -,\ i_{j+1} = +\}$, $\mathcal{I}^0$ denote the set of indexes corresponding to the first point of a segment of constant curvature, i.e. $\mathcal{I}^0 = \{j : i_j = 0,\ i_{j-1} \neq 0\}$.

The following algorithm provides the optimal velocity profile for minimum time travel along the path $\mathcal{P}_{AB}$.

ALGORITHM FOR OPTIMAL VELOCITY PROFILE

- From (z_1^A, z_2^A) integrate the equations of motion (9) forward in time with $u = +1$ to construct the characteristic $Z_A^+(z_1)$.
- From (z_1^B, z_2^B) integrate the equations of motion (9) backward in time with $u = -1$ to construct the characteristic $Z_B^-(z_1)$.
- For each point of minimum radius P_k, $k \in \mathcal{I}^{\mp}$, construct the following characteristics: the characteristic $Z_{P_k}^-(z_1)$ by integrating (9) backward in time from $(z_1^{P_k}, z_{2\text{crit}}(z_1^{P_k}))$ using $u = -1$, and the characteristic $Z_{P_k}^+(z_1)$ by integrating (9) forward in time from $(z_1^{P_k}, z_{2\text{crit}}(z_1^{P_k}))$ using $u = +1$.
- For each segment $\mathcal{P}^0_{P_\ell P_{\ell+1}}$ of constant radius $R(z_1) = R_\ell$ where $\ell \in \mathcal{I}^0$, construct the following characteristics: the characteristic $Z^0_{P_\ell P_{\ell+1}}(z_1)$ of constant velocity equal to $z_{2\text{crit}}^{P_\ell} = \sqrt{|R_\ell|}$, the characteristic $Z_{P_\ell}^-(z_1)$ by integrating backward in time from $(z_1^{P_\ell}, z_{2\text{crit}}^{P_\ell})$ using $u = -1$, and the characteristic $Z_{P_{\ell+1}}^+(z_1)$ by integrating forward in time from $(z_1^{P_{\ell+1}}, z_{2\text{crit}}^{P_\ell})$ using $u = +1$.
- The solution to the minimum time problem is given by

$$z_2^*(z_1) = \min\left\{ Z_A^+(z_1), Z_B^-(z_1), Z_{P_k}^-(z_1), Z_{P_k}^+(z_1), Z^0_{P_\ell P_{\ell+1}}(z_1), Z_{P_\ell}^-(z_1), Z_{P_{\ell+1}}^+(z_1) \right\}, \tag{40}$$

where $k \in \mathcal{I}^{\mp}$ and $\ell \in \mathcal{I}^0$.

Proof of optimality can be easily provided by showing that the previous solution maximizes pointwise the velocity. We demonstrate this fact in the following example.

8.1 Example (General Solution)

Consider the path $\mathcal{P}_{AB}$ shown in Fig. 6(a). We can identify points of minimum radius at P_1, P_4 and P_9 ($\mathcal{I}^{\pm} = \{1, 4, 9\}$), and intervals of constant radius $\mathcal{P}_{P_5P_6}$ and $\mathcal{P}_{P_7P_8}$ ($\mathcal{I}^0 = \{5, 7\}$). Figure 6(b) shows the construction of the necessary characteristics using the rules of the previous section. The minimum time solution is given by (40) and it is shown in Fig. 7(a).

Consider now the intervals (i) - (viii) along the optimal solution as in Fig. 7(b). In the interval (i) we use maximum acceleration $u = +1$ from the starting point A and thus the velocity is maximized point-wise in the interval (i). In (ii) the vehicle decelerates with $u = -1$ towards the critical velocity at P_4. A trajectory passing from a point of higher velocity in (ii) would violate the constraint (35) at P_4. After P_4 we have maximum acceleration and thus point-wise maximum velocity in (iii). The velocity in (iv) is equal to the maximum allowable from (35). In (v) we have maximum acceleration and thus maximum velocity as in (iii). Point-wise maximality of the velocity in (vi) and (vii) is shown in accordance to (ii) and (iii) respectively. Considering the problem from B to A, the trajectory in (viii) corresponds to maximum acceleration from the fixed condition at B and thus it maximizes the velocity point-wise.

We conclude that the velocity is maximized point-wise throughout the trajectory from A to B, and thus the trajectory computed using (40) is the solution to the minimum time problem.

9 Application to an F1 circuit

In this section we validate the proposed methodology by applying it to an actual road track. Specifically, we use the previous methodology in order to generate the velocity profile for the Silverstone F1

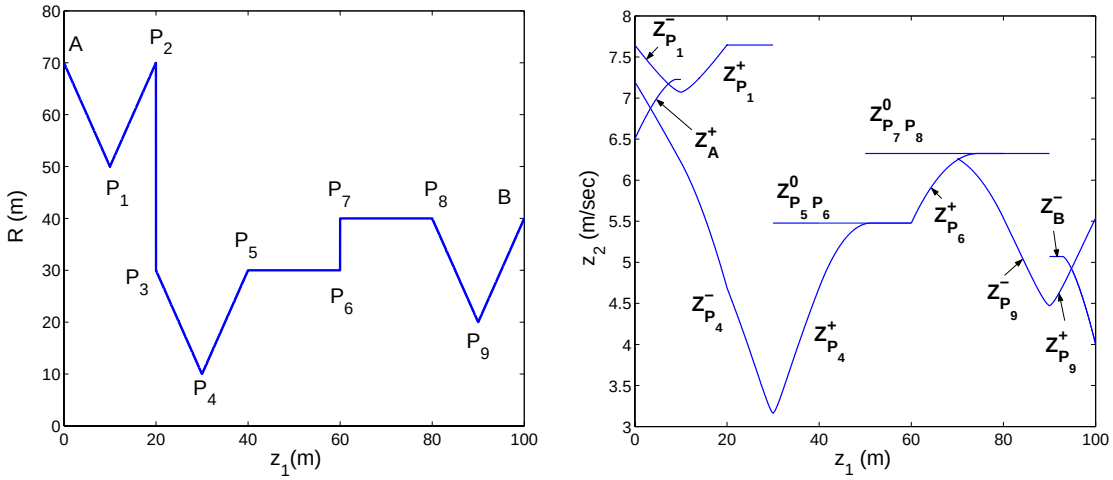

(a) (b)

Figure 6: (a) A general case radius profile path; (b) the free boundary conditions problem solutions for constant radius and min R subarcs.

circuit [12], given the acceleration limits of a typical F1 race car. Based on the performance characteristics of the vehicles in [2] and [12], we can write the equations of motion for an F1 car (including the effect of aerodynamic drag) as follows (compare with (5))

$$\dot{v} = \frac{f_t}{m} - \alpha v^2, \qquad v^2 = \frac{f_n}{m} r(s) \tag{41}$$

where we assume the following maximum tire acceleration and deceleration values

$$f_t^{\max}/m = 16 \text{ m/sec}^2, \qquad f_t^{\min}/m = -18 \text{ m/sec}^2,$$

in the longitudinal direction, and

$$f_n^{\max}/m = \pm 30 \text{ m/sec}^2$$

in the lateral direction. The coefficient of the aerodynamic drag is given by $\alpha = 0.0021$.

For simplicity, in (41) we have neglected the engine limitations and aerodynamic down-force effects (and ground effect). The deceleration due to aerodynamic drag is included in these equations since for F1 cars (because of their extremely high speeds) this effect is significant and cannot be ignored. The effect of the aerodynamic drag is to reduce the maximum available acceleration in the longitudinal direction at each instant of time. This is in addition to the reduction stemming from the necessary centripetal acceleration to remain on the track (see equation (6)). The net result is therefore a reduction of the available acceleration envelope in the longitudinal direction, along with a similar increase of the possible deceleration.

The velocity profile generated using the proposed approach for the Silverstone circuit is shown in Fig. 8(b). For comparison, Fig. 8(a), taken from [12], shows velocity measurements for three laps of an F1 car along the Silverstone circuit. Despite the simplifying assumptions used in our mathematical model, the correlation between the two plots of Fig. 8 is remarkable. These results provide a strong indication for the validity of the proposed strategy for constructing optimal, or close to optimal, velocity profiles along a given path for real-life problems. Furthermore, they provide strong evidence for the common belief that expert F1 drivers – through experience and repeated testing – have developed optimization strategies that are very close (if not identical) to optimal ones as dictated by the physics of the problem.

The calculated lap time using the approach of Section 8 is 82.7 sec. The measured lap times corresponding to the data of Fig. 8(a) are 86.063 sec, 90.891 sec and 85.805 sec respectively for each lap.

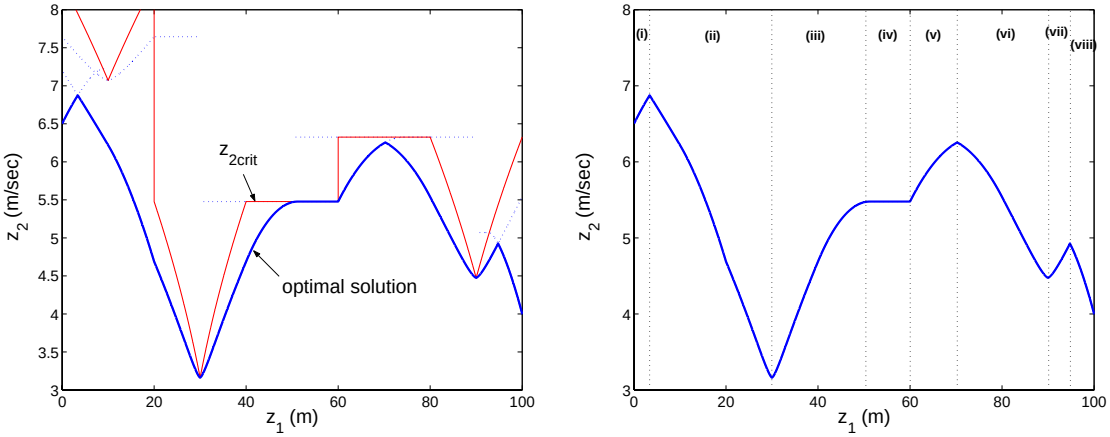

(a) (b)

Figure 7: Optimal velocity profile for the general case path of Fig. 6.

Incidentally, we note that the record time for the Silverstone circuit belongs to K. Raikkonen (78.233 sec, McLaren Mercedes, 2004).

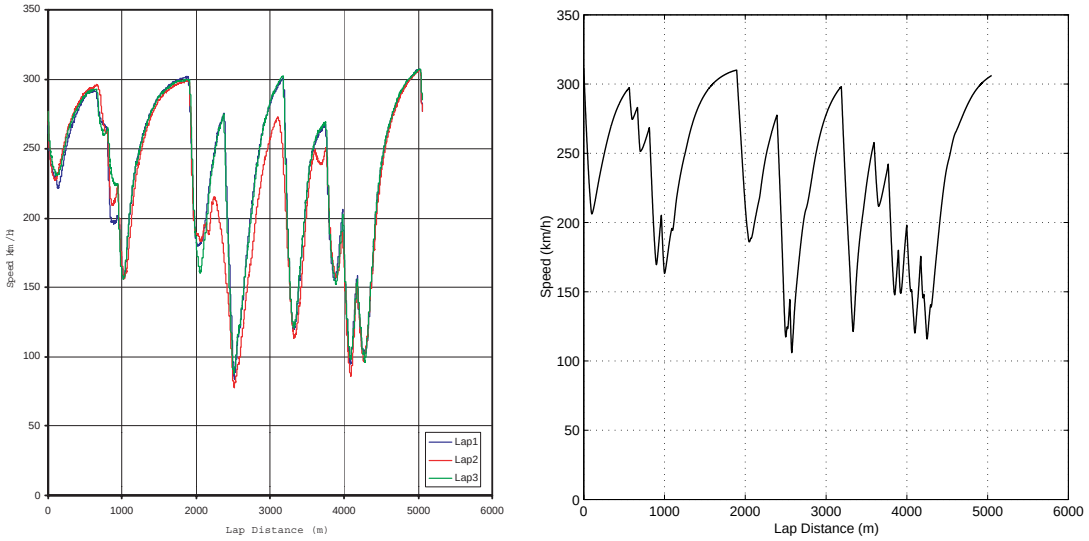

(a) (b)

Figure 8: Velocity profiles through the Silverstone circuit: (a) achieved by human driver, (b) computed velocity profile using the approach of Section 8.

10 Receding Horizon Implementation

When the environment is changing the optimal profile needs to be generated on-line. One way to achieve this, is for the trajectory optimization to be implemented in a receding horizon scheme rather than executed in one shot, from the start point to the end point [13, 14, 15]. Below we propose a receding horizon scheme to adaptively choose the planning and execution horizons to provide guaranties that the velocity will not exceed the critical value at any point, and that there exists an "escape plan" at the end

of each optimization step.

10.1 Receding Horizon Scheme

Figure 9 demonstrates how the receding horizon scheme works. The *Planning Horizon* (PH_i) is the distance from the current position up to the point which the i^{th} optimization step is performed. The *Execution Horizon* (EH_i) is a fraction of PH_i and it is the distance up to the point which the planned optimization will actually be executed. When the vehicle reaches the *Replanning Horizon* RH_i, which is a fraction of EH_i, the optimization is performed again up to the new planning horizon PH_{i+1}.

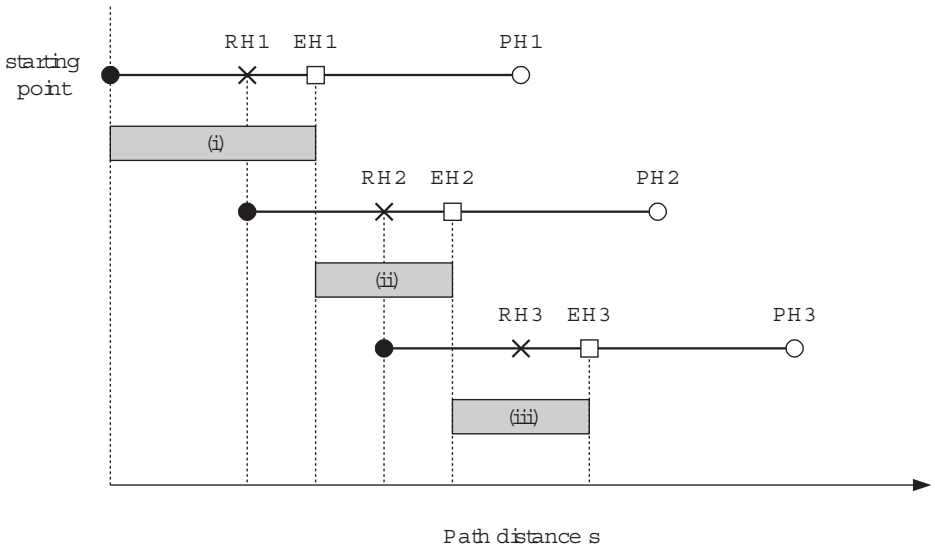

Figure 9: Optimization with receding horizon.

Let the vehicle be at the starting point ($s = s_0$ in Fig. 9). The optimization methodology is applied up to PH_1. After the optimization is completed, the vehicle may start executing the optimal trajectory up to EH_1. The shadowed area (i) in Fig. 9 shows the portion of the first optimization that is actually executed. When the vehicle reaches RH_1 the optimization is applied again from the current position RH_1 to the new planning horizon PH_2. The portion of the second optimization that will be actually executed is from EH_1 to EH_2 and it is shown as the shadowed area (ii) in Fig. 9. The process will end when the final destination is within the execution horizon. The distance between RH_i and EH_i is chosen such that enough time is allowed for the computation of the optimal trajectory from RH_i to PH_{i+1} before EH_i is reached. If the computation is instantaneous RH_i and EH_i can coincide.

10.2 Robustness Guarantees

In this section we propose a dynamic scheme to determine planning and execution horizons in the z_1 domain and guarantee the existence of an "escape plan" in the end of each executed subarc. We propose the following formula to determine the planning horizon of the i^{th} optimization step

$$\mathrm{PH}_i = \max\{Tv_i, \mathrm{PH}_{\min}\}, \tag{42}$$

where v_i is the vehicle velocity at the position of the execution horizon of the previous optimization step EH_{i-1}, $v_i = z_2(\mathrm{EH}_{i-1})$, T is a constant "reaction" time, and $\mathrm{PH}_{\min}$ is the minimum planning horizon (typically for $v_i = 0$). At the initial point A on the path, for the first optimization step $i = 1$ we have

$\mathrm{EH}_0 = z_1^A$. The optimal solution from the current position EH_{i-1} to PH_i is calculated using (40) and is denoted by ${}^i z_2^*(z_1)$.

Next, we construct the characteristic from $(z_1 = \mathrm{PH}_i, z_2 = 0)$ integrating backwards in time using $u = -1$. This characteristic is denoted by ${}^i z_2^{\mathrm{esc}}(z_1)$ and is referred to as *escape trajectory* of the i^{th} optimization step. We choose the execution horizon for the i^{th} optimization step as follows:

$$\mathrm{EH}_i = \left\{ z_1 : \ {}^i z_2^*(z_1) = \ {}^i z_2^{\mathrm{esc}}(z_1), \ z_1 \in [\mathrm{EH}_{i-1}, \mathrm{PH}_i] \right\}. \tag{43}$$

In the case when

$$\{(z_1, {}^i z_2^*(z_1)), z_1 \in [\mathrm{EH}_{i-1}, \mathrm{PH}_i]\} \bigcap \{(z_1, {}^i z_2^{\mathrm{esc}}(z_1)), z_1 \in [\mathrm{EH}_{i-1}, \mathrm{PH}_i]\} = \varnothing, \tag{44}$$

we need to increase T in (42) to determine a longer planning horizon until we can find the intersection point of the optimal solution and the escape trajectory (43).

At the end of each executed subarc EH_i we optimize up to the new planning horizon PH_{i+1}. The vehicle can decelerate enough to negotiate any corner outside PH_i since we have guaranteed that the vehicle starting from EH_i can come to a complete stop at PH_i. In case an obstacle exists after PH_i the vehicle can follow the escape trajectory to avoid collision. The Receding Horizon optimization scheme terminates when the end point B is within the execution horizon, namely $z_1^B \leq \mathrm{EH}_i$ for some i.

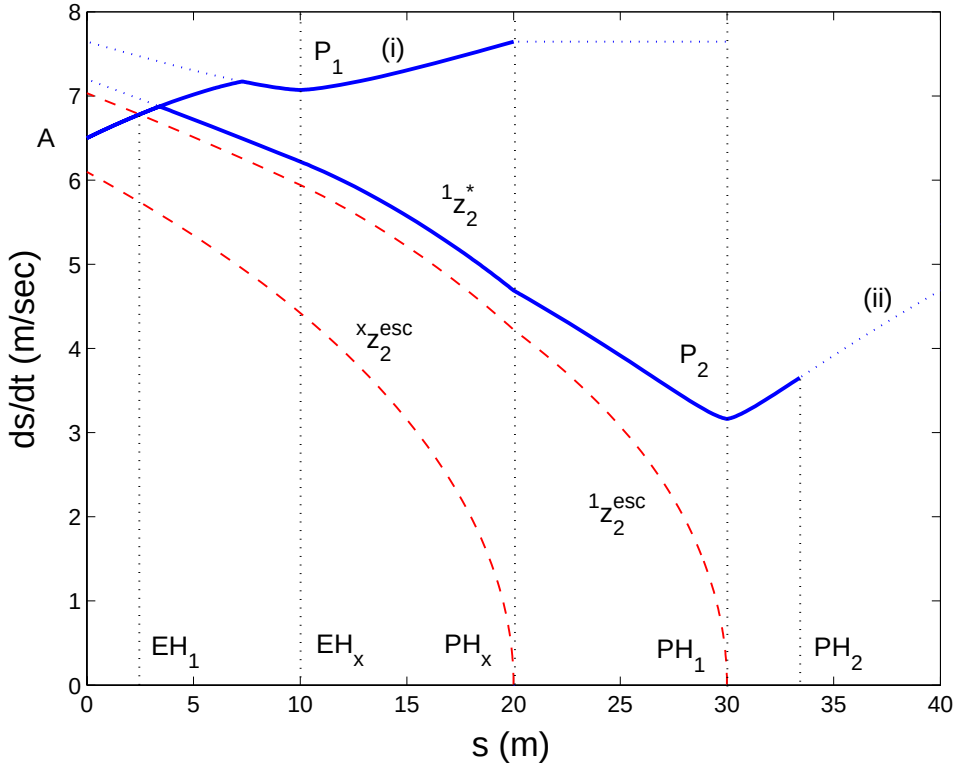

Figure 10: Dynamic scheme for determination of EH_i.

10.3 Numerical Example (Receding Horizon Implementation)

In this section we apply the proposed receding horizon algorithm to the F1 car trajectory of Section 9. We have chosen $T = 5$ sec, which for this example is enough for the "emergency stop" characteristic to

intersect the optimal solution within the planning horizon for each iteration. The minimum planning horizon was chosen as $\mathrm{PH}_{\min} = 200$ m.

In Fig. 11 the results of the first five steps of the receding horizon scheme are shown, along with the planning and execution horizons of each step. The solution (solid line) is compared with the infinite-horizon solution of the optimal velocity generator of Section 9 (dotted line). The two solutions coincide, thus confirming the validity of the proposed receding horizon scheme.

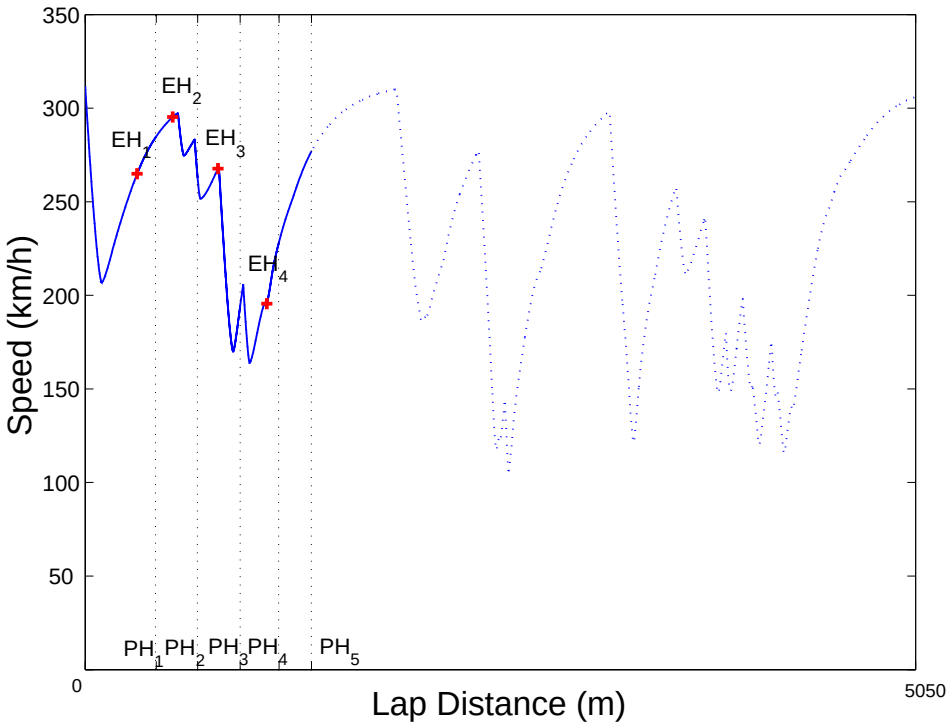

Figure 11: Optimization with receding horizon for the Silverstone circuit.

11 Conclusions

In this work we have presented a constructive proof of optimality for generating velocity profiles for minimum time travel of vehicles along prescribed paths. The limitations from the allowable magnitude and direction of the friction forces are explicitly accounted for. The necessary optimality conditions are derived, which provide the number and type of control switchings according to the geometry of the prescribed path. The whole approach is analytic, requiring only quadratures and thus it can be easily implemented on-line. A receding horizon scheme has also been proposed to lower the computational cost of implementing the proposed approach and to account for unpredictable changes in the environment. Numerical simulations show that the proposed on-line velocity optimizer is competitive when compared to lap times obtained by expert F1 race drivers.

References

[1] Hendrikx, J., Meijlink, T., and Kriens, R., *Application of Optimal Control Theory to Inverse*

Simulation of Car Handling, Vehicle System Dynamics, Vol. 26, pp. 449–461, 1996.

[2] Casanova, D., Sharp, R. S., and Symonds, P., *Minimum Time Manoeuvring: The Significance of Yaw Inertia*, Vehicle System Dynamics, Vol. 34, pp. 77–115, 2000.

[3] Casanova, D., Sharp, R. S., and Symonds, P., *On Minimum Time Optimisation of Formula One Cars: The Influence of Vehicle Mass*, in Proceedings of AVEC 2000, Ann-Arbor, MI, August 22-24 2000.

[4] Velenis, E., and Tsiotras, P., *Minimum Time vs Maximum Exit Velocity Path Optimization During Cornering*, in 2005 IEEE International Symposium on Industrial Electronics, Dubrovnic, Croatia, pp. 355–360, June 2005.

[5] Spenko, M., *Hazard Avoidance for High-Speed Rough-Terrain Unmanned Ground Vehicles*. PhD thesis, Department of Mechanical Engineering, Massachusetts Institute of Technology, 2005.

[6] Metz, D., and Williams, D., *Near Time-Optimal Control of Racing Vehicles*, Automatica, Vol. 25, No. 6, pp. 841–857, 1989.

[7] Gadola, M., Vetturi, D., Cambiaghi, D., and Manzo, L., *A Tool for Lap Time Simulation*, in Proceedings of SAE Motorsport Engineering Conference and Exposition, Dearborn, MI, 1996.

[8] Lepetic, M., Klancar, G., Skrjanc, I., Matko, D., and Potocnic, B., *Time Optimal Path Planning Considering Acceleration Limits*, Robotics and Autonomous Systems, Vol. 45, pp. 199–210, 2003.

[9] Bobrow, J., Dubowsky, S., and Gibson, J., *On the Optimal Control of Robotic Manipulators with Actuator Constraints*, in Proceedings of the American Control Conference, San Francisco, CA, pp. 782–787, June 1983.

[10] Bobrow, J., Dubowsky, S., and Gibson, J., *Time-Optimal Control of Robotic Manipulators Along Specified Paths*, International Journal of Robotics Research, Vol. 4, No. 3, pp. 3–17, 1985.

[11] Shin, K., and McKay, N., *Minimum-Time Control of Robotic Manipulators with Geometric Path Constraints*, IEEE Transactions on Automatic Control, Vol. 30, No. 6, pp. 531–541, 1985.

[12] Anonymous, Inertial and GPS Measurement System, Report from Silverstone F1 Test, Technical Report, Oxford Technical Solutions, Oxfordshire, UK, 2002.

[13] Schouwenaars, T., De Moor, B., Feron, E., and How, J., *Mixed Integer Programming for Multi-Vehicle Path Planning*, in Proceedings of the 2001 European Control Conference, Porto, Portugal, pp. 2603–2608, September 2001.

[14] Bellingham, J., Richards, A., and How, J., *Receding Horizon Control of Autonomous Aerial Vehicles*, in Proceedings of the American Control Conference, Anchorage, AK, pp. 3741–3746, May 8-10 2002.

[15] Schouwenaars, T., Feron, E., and How, J., *Safe Receding Horizon Path Planning for Autonomous Vehicles*, in Proceedings of the 40th Allerton Conference on Communication, Control and Computing, Monticello, IL, October 2002.

List of Figures